Gold Bull (2014) 47:275–282
DOI 10.1007/s13404-014-0152-y

ORIGINAL PAPER

Alumina hollow microspheres supported gold catalysts for low-temperature CO oxidation: effect of the pretreatment atmospheres on the catalytic activity and stability

Yu-Xin Miao · Lei Shi · Li-Na Cai · Wen-Cui Li

Published online: 17 September 2014

Abstract Hierarchically organized γ-Al_2O_3 hollow microspheres were prepared via a hydrothermal method using potassium aluminum sulfate and urea as reactants. The corresponding Au/Al_2O_3 catalysts were obtained using a deposition-precipitation (DP) method. The effect of the pretreatment under different atmospheres (N_2, air, and H_2) on the activity and stability of the Au/Al_2O_3 catalysts in CO oxidation was investigated. The results showed that the pretreatment under H_2 atmosphere improved the low-temperature CO oxidation activity. Furthermore, a 50 h long-term test at 30 °C showed no significant deactivation for the H_2-pretreated catalyst. Moreover, the catalytic activity was promoted by H_2O vapor in all cases, and the H_2-pretreated catalyst exhibited a good tolerance in the co-presence of CO_2 and H_2O. Finally, oxygen temperature-programmed desorption (O_2-TPD) and in situ diffuse reflectance infrared Fourier transform spectra (DRIFTS) revealed that the reductive atmosphere pretreatment greatly improved the CO adsorption capacity and facilitated the oxygen activation.

Keywords Pretreatment atmosphere · CO oxidation · Gold catalyst · Stability · DRIFTS

Introduction

Supported gold nanoparticles (Au NPs) have been intensively studied in catalysis [1], particularly for the low-temperature CO oxidation [2–6], water-gas shift (WGS) reaction [7], VOC removal [8], and selective oxidation of organic compounds [9]. It is generally considered that the catalytic activity of Au NPs is strongly dependent on the size (<5 nm) and morphology [10–12]. The Au NPs supported on reducible oxides such as Fe_2O_3 [13], TiO_2 [14], and CeO_2 [15] may have smaller sizes and present higher catalytic performance compared to non-reducible oxide materials (SiO_2 [16], Al_2O_3 [17]). Generally, the strong interaction between Au NPs and the reducible oxide supports helps to stabilize small Au NPs and also increases the catalytic activity [18]. However, we reported that the alumina nanosheets with rough surface can efficiently stabilize the Au NPs and thus contribute a high activity for CO oxidation [19].

Besides the nature of supports [20, 21], it is believed that the pretreatment process of the Au catalyst can strengthen the interaction between Au and the supports, and so improve the CO oxidation activity [22, 23]. Wang et al. [24] prepared a series of Au/α-Mn_2O_3 catalysts by a deposition-precipitation method and found that the best activity was obtained when the catalyst was pretreated with O_2 because a specific formed oxygen-enriched interface gave enhanced metal-support synergy. On the contrary, the Au/α-Mn_2O_3 catalysts pretreated with He and H_2 had inferior catalytic activities on account of severe deactivation and over-reduction of the surface of support, respectively. In the work of Xu et al. [25], a highly active "NiO-on-Au" nanocatalyst was synthesized using a two-step method. They suggested that the catalyst pretreated with H_2 had a better catalytic performance since the formed NiO-Au boundaries can provide dual sites for O_2 activation and CO adsorption. Our recent work also confirmed that the pretreatment atmospheres significantly influence the catalytic activity of the Au/CeO_2 catalyst for CO oxidation [26]. The characterization results showed that pretreatment can significantly change the surface interaction between Au species and CeO_2 support.

However, concerning the influence of the pretreatment atmospheres on the catalytic activity, current studies mainly

Y.-X. Miao · L. Shi · L.-N. Cai · W.-C. Li (✉)
State Key Laboratory of Fine Chemicals, School of Chemical Engineering, Dalian University of Technology, Dalian 116024, People's Republic of China
e-mail: wencuili@dlut.edu.cn

revolve around the reducible-oxide-supported Au catalysts. There were few studies in terms of the non-reducible-oxide-supported Au NPs. In the present work, we take the home-made highly active Au/Al_2O_3 catalyst as an example and study the effect of the pretreatment atmospheres on the activity towards CO oxidation. In addition, the stability of the pretreated Au/Al_2O_3 catalyst under CO_2 and H_2O steam was also conducted. The oxygen temperature-programmed desorption (O_2-TPD) and in situ diffuse reflectance infrared Fourier transform spectra (DRIFTS) characterization were performed to investigate the surface characteristics of the pretreated Au/Al_2O_3 catalyst with the aim of correlating with the catalytic behavior.

Experimental

Catalyst preparation

Alumina hollow microspheres were prepared using a hydrothermal method [27]. In detail, 5 mmol of $KAl(SO_4)_2{\cdot}12H_2O$ was dissolved in 50 mL of deionized water, and then 10 mmol of $CO(NH_2)_2$ dissolved in 50 mL of deionized water was added into the $KAl(SO_4)_2{\cdot}12H_2O$ solution under vigorous stirring at room temperature for 0.5 h. The mixture was transferred into a Teflon-lined stainless steel autoclave and heated at 180 °C for 3 h. After thorough washing and centrifugation, the solid was dried at 80 °C and calcined at 600 °C in a muffle oven for 2 h.

Gold was deposited onto the surface of γ-Al_2O_3 hollow microspheres by a deposition-precipitation (DP) method using $(NH_4)_2CO_3$ as precipitant and $HAuCl_4$ solution (7.888 g/L) as the gold precursor, similar to the procedure used in our previous work [28]. In a typical preparation, $HAuCl_4$ was added dropwise to an aqueous suspension of Al_2O_3, and the pH of the suspension was adjusted to 8–9 by addition of 0.5 M $(NH_4)_2CO_3$ solution at 60 °C for 2 h. Afterwards, the product was washed several times with deionized water until it was clear of Cl^- (tested by $AgNO_3$), followed by centrifugal separation and drying under vacuum. The theoretical content of Au is 1 wt%. Prior to the catalytic test, the samples were pretreated under flowing N_2, 14 vol% H_2/N_2 and air atmospheres at 250 °C for 2 h, and the corresponding samples were named Au/Al_2O_3-N_2, Au/Al_2O_3-H_2, and Au/Al_2O_3-air, respectively.

Catalyst characterization

The morphology of the Al_2O_3 sample was observed using a Hitachi S4800 scanning electron microscope (SEM) operated at 20 kV. Transmission electron microscope (TEM) images were obtained with a FEI Tecnai G220 S-Twin microscope. The X-ray diffraction (XRD) pattern was collected on a Siemens D/Max 2400 X-ray powder diffractometer (Cu K_α radiation, λ=1.54056 Å) with a working voltage of 40 kV and a current of 100 mA. The Brunauer-Emmett-Teller (BET) surface area of the Al_2O_3 sample was measured by N_2 adsorption at −196 °C on a Micromeritics Tristar 3000 instrument. The samples were degassed at 200 °C for 4 h prior to analysis. In situ DRIFTS were recorded by a Nicolet 6700 spectrometer equipped with MCT detector and KBr window. The Au/Al_2O_3 catalyst was heated to 200 °C for 2 h under vacuum prior to the test. The background spectrum was collected in a flowing He atmosphere at RT (30 °C), and in situ DRIFTS were collected in 5 vol% CO/N_2 or 1 vol% CO/air atmosphere for 20 min. O_2-TPD experiments were conducted on a Micromeritics Autochem II 2920 apparatus. The Au/Al_2O_3 catalyst was first treated in an Ar flow at 200 °C for 2 h. After cooling to 30 °C, the pretreated sample was exposed to O_2 for 1 h and heated to 800 °C, with a heating rate of 10 °C/min. The actual loading of Au was determined using an inductively coupled plasma atomic emission spectrometer (ICP-AES) on the Optima 2000 DV.

Catalytic test

The activity of the Au/Al_2O_3 catalyst for CO oxidation was evaluated with a fixed-bed flow quartz reactor (8 mm i.d.). A typical flow rate was 1 vol% CO and 20 vol% O_2 in N_2 (79 vol%), giving a total flow rate of 67 mL/min. The catalyst sample was 100 mg, and the corresponding space velocity was 40,000 mL/h g_{cat}. The composition of the effluent gas was analyzed using an online GC-7890 gas chromatograph equipped with a thermal conductivity detector (TCD) and a 5A molecular sieve column (T=80 °C, H_2 as the carrier gas).

Results and discussion

Alumina hollow microspheres

In Fig. 1a–c, the SEM and TEM images of the obtained sample display hollow microsphere structures with a diameter of 4–6 μm and a shell thickness of 600–700 nm. The spheres consist of closely packed nanoflakes. The main diffraction peaks of alumina are present at 2θ=31.9° (220), 37.3° (311), 45.7° (400), and 66.9° (440) (Fig. 1d), which can be assigned to the γ-alumina crystalline phase (JCPDS card 10-0425). The BET specific surface area and the pore volume of Al_2O_3 were calculated as 209 m^2/g and 0.66 cm^3/g, respectively. These results are similar to our recent work [27]. The actual Au content is 0.53 wt% by ICP measurement.

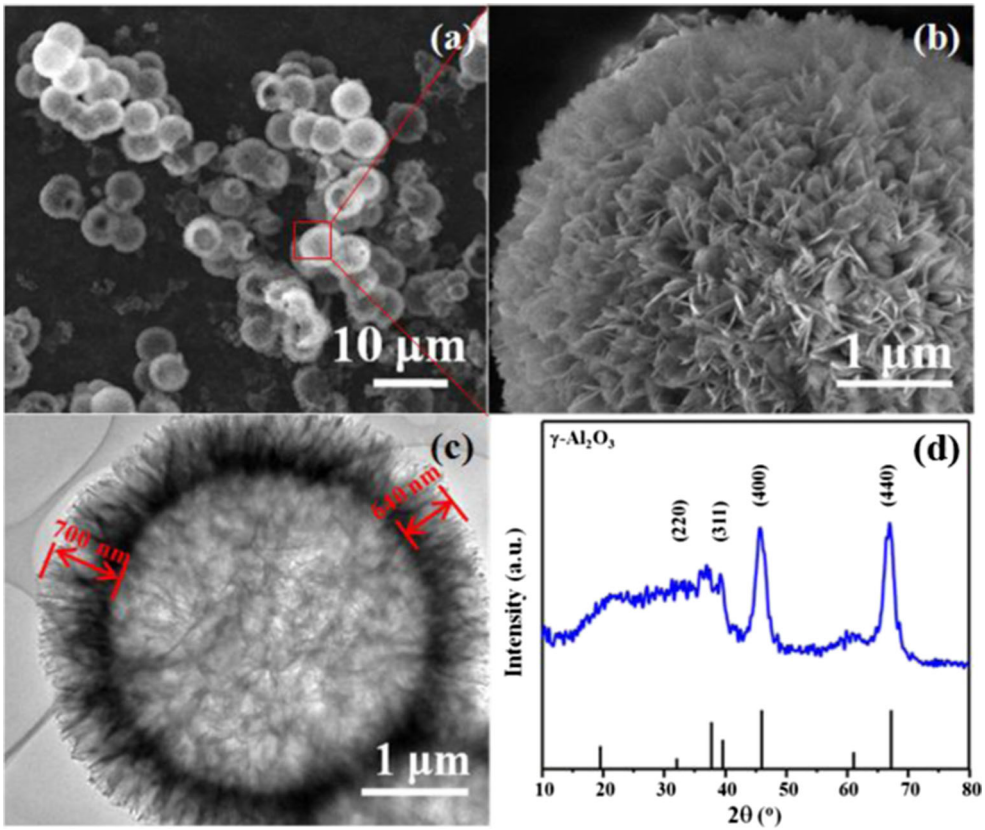

Fig. 1 **a**, **b** SEM images, **c** TEM image, and **d** XRD patterns of the Al_2O_3 sample

Catalytic activities and stabilities

Figure 2 gives the CO oxidation performance over the Au/Al_2O_3 catalysts pretreated under different atmospheres. The initial CO conversion of Au/Al_2O_3-H_2 is 62 % at 30 °C, which is significantly higher than those of Au/Al_2O_3-air and Au/Al_2O_3-N_2 catalysts under the same reaction conditions. Moreover, a complete conversion can be obtained for the Au/Al_2O_3-H_2 at a low temperature of 60 °C. In contrast, the Au/Al_2O_3-air catalyst showed a slightly increased initial activity, but a lower activity at high temperature compared to the Au/Al_2O_3-N_2 catalyst. In addition, based on the best results from Fig. 2, the reactive rate at 30 °C for the Au/Al_2O_3-H_2 catalyst was calculated as 2.109 mol/h g_{Au}, which is comparable and even higher than the results in the literature [19, 28–30] (Table 1).

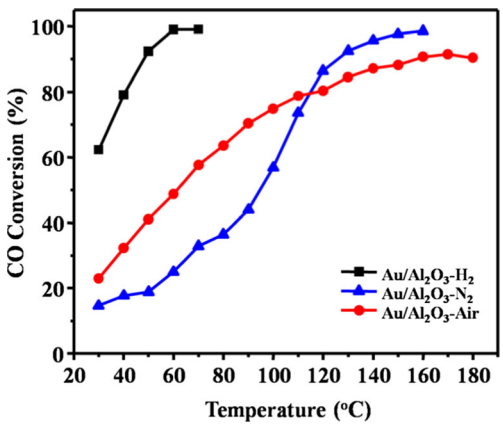

Fig. 2 CO conversions as a function of reaction temperature over Au/Al_2O_3 catalysts with different pretreatment atmospheres

The stabilities of the Au/Al_2O_3 catalysts pretreated under different atmospheres in CO oxidation were measured at 30 °C. As shown in Fig. 3a, the conversion of CO over the Au/Al_2O_3-H_2 catalyst increased from 62 % in the initial time to 75 % in 10 h and then maintained an excellent stability over 50 h on stream. The Au/Al_2O_3-air and Au/Al_2O_3-N_2 catalysts also exhibit stable catalytic performances, but the CO conversions were only 27 and 7 %, respectively. It is evident that the CO oxidation activities and stabilities over the Au/Al_2O_3 catalysts are sensitive to the pretreatment atmospheres. The possible explanation is supplied in the following by means of in situ DRIFTS characterization.

Furthermore, the effects of the H_2O vapor and CO_2 with varied concentration on the stability of the Au/Al_2O_3-H_2 catalyst were also tested. As expected, it can be observed in Fig. 3b that the CO conversion increased when the concentration of H_2O vapor was raised. The CO conversion of the Au/Al_2O_3-H_2 catalyst under 500 ppm of H_2O vapor at 30 °C is ~70 % and increased to ~87 % under 5000 ppm. As a result, complete CO conversion is achieved at lower temperatures

Table 1 Comparison of catalytic performances with other reported Au NPs

Catalysts	Au loading (wt%)[a]	Composition of feed gas (vol%)		Space velocity	$T_{100\ \%}$ (°C)[b]	T (°C)[c]	TOF (/s)[d]	Rate (mol/h g_{Au})	Stability test (h)	Reference
		CO	O_2							
Au/Al_2O_3	0.53	1	20	40,000 mL/h g_{cat}	60	30	0.096	2.109	50	This work
Au/Al_2O_3	2.4	1	20	80,000 mL/h g_{cat}	2	0	0.141	1.433	–	[19]
Au/Al_2O_3	2.08	1	20	80,000 mL/h g_{cat}	10	20	0.0878	1.604	–	[28]
Au/Al_2O_3	1.0	1	20	15,000/h	40	25	0.25	1.62	–	[29]
Au/Al_2O_3	0.065	1	0.5	20,000 mL/h g_{cat}	24	24	–	1.803	0.5	[30]
Au/Fe-La -Al_2O_3	1	1	20	16,000 mL/h g_{cat}	−10	25	–	0.48	30	[31]
$Au/FeO_x/Al_2O_3$	1.35	1	10	45,000/h	30	–	–	–	30	[32]
Au-Rh/Al_2O_3	0.94	0.2	20	54,000/h	0	–	–	–	33	[33]

[a] The actual loadings of Au were determined by ICP technique

[b] $T_{100\ \%}$ represents the temperatures for 100 % CO conversion

[c] The temperature of the corresponding reactive rate and TOF of Au catalysts were calculated

[d] Turnover frequency (TOF) was calculated based on the number of supported Au atoms

(30 °C) under 10,000 ppm of H_2O vapor. However, with the addition of CO_2 (Fig. 2c), the catalyst suffers from a rapid decrease in the activities of CO oxidation; for example, CO conversion is approximately 40 % with the addition of 15 and 20 % CO_2. A possible explanation is that the increase in CO_2 concentration leads to the formation of carbonate-like species and/or the competitive adsorption of CO_2 on the active sites which inhibit the oxygen mobility. Figure 2d gives the corresponding CO conversion curves in the co-presence of H_2O and CO_2 at 30 °C. It is seen that the Au/Al_2O_3-air and Au/Al_2O_3-H_2 catalysts gave transient 100 % CO conversion after which the catalytic activities gradually decreased and reached a stable activity of 90 %. In contrast, low catalytic activities occurred with the Au/Al_2O_3-N_2 catalyst under the same

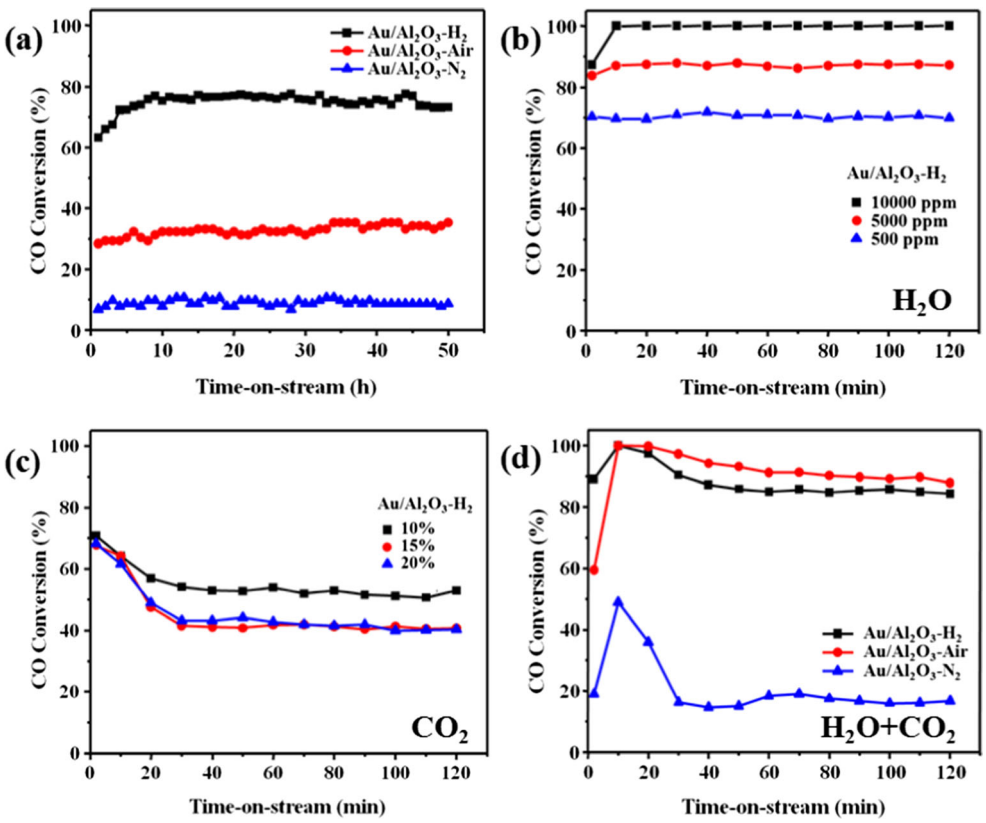

Fig. 3 **a** The stabilities of various Au/Al_2O_3 catalysts for the CO oxidation at 30 °C. **b** Au/Al_2O_3-H_2 catalyst in the presence of H_2O vapor at 30 °C. **c** Au/Al_2O_3-H_2 catalyst in the presence of CO_2 at 30 °C. **d** Au/Al_2O_3 catalysts for the CO oxidation in the co-presence of 10,000 ppm H_2O and 15 % CO_2 at 30 °C (reaction conditions: 1 vol% CO, 20 vol% O_2, 15 vol% CO_2, 1 vol% H_2O, and balance N_2. WHSV, 40,000 mL/h g_{cat})

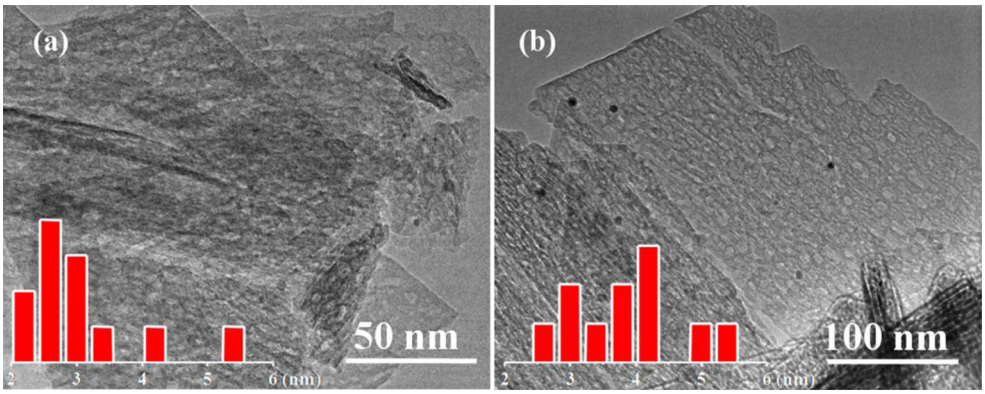

Fig. 4 **a** TEM image of a fresh Au/Al_2O_3-H_2 catalyst. **b** TEM image of a used Au/Al_2O_3-H_2 catalyst

reaction conditions. The noticeable promotion of initial activity for Au/Al_2O_3-air and Au/Al_2O_3-N_2 catalysts may be considered to be moisture-assisted oxygen activation [34]. These results indicate a promoting effect of reductive or oxidative atmosphere pretreatment on the activity of the Au/Al_2O_3 catalysts under the co-presence of H_2O vapor and CO_2.

In order to investigate the stability of Au NPs after treatment, one representative Au/Al_2O_3-H_2 catalyst was characterized by TEM (Fig. 4a, b). One can see that the gold particle sizes of the used Au/Al_2O_3-H_2 catalyst (3.9±0.4 nm) are similar to those of the fresh sample (3.0±0.4 nm). The outstanding stability could be relating to the novel surface structure of our Al_2O_3 support, which contributes to a solid stabilization of Au NPs [19, 28].

CO adsorption on the Au/Al_2O_3 catalyst

To study the initial surface property of various Au/Al_2O_3 catalysts, we chose CO as a probe molecule and employed in situ DRIFTS to study the adsorption on the catalyst surface at 30 °C. As shown in Fig. 5, when the Au/Al_2O_3 catalysts were exposed to CO for 20 min at 30 °C, several bands at 1440, 1560, 1641, 2056, 2114, and 2171 cm^{-1} were observed. Concomitant with the CO adsorption, the peaks in the 1400–1800 cm^{-1} region are related to the vibration of carbonate-like species as suggested by other studies [35, 36]. The absorption band at 2056 cm^{-1} in our study was also observed by Liu et al. [37] at 2048 cm^{-1}, which is assigned to negatively charge gold carbonyls [38]. At the same time, one weak absorption band at 2114 cm^{-1} can be assigned to Au^0–CO. On the other hand, the band at 2171 cm^{-1} can be attributed to $Au^{\delta+}$–CO [39]. There are no striking differences between the peak position of $Au^{\delta+}$/Au^0–CO for Au/Al_2O_3 catalysts with different pretreatment atmospheres. This result indicates that the co-presence of $Au^{\delta+}/Au^0$ on the surface of Au/Al_2O_3 catalysts [27] and the pretreatment atmospheres had little effect on CO adsorption on the surface of the Au/Al_2O_3 catalyst.

Oxygen temperature-programmed desorption

To gain the adsorption/desorption capacity of oxygen on the catalyst surface, O_2-TPD measurements were carried out. The O_2-TPD profiles of the Au/Al_2O_3 catalysts pretreated under different atmospheres are shown in Fig. 6. The oxygen desorption peaks of Au/Al_2O_3-N_2, Au/Al_2O_3-air, and Au/Al_2O_3-H_2 are 71, 69, and 59 °C, respectively, which can be ascribed to the decomposition of Au_2O_3 or surface oxygen species

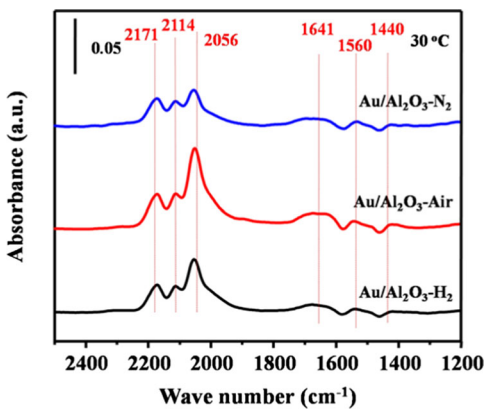

Fig. 5 In situ DRIFTS of various Au/Al_2O_3 catalysts after CO adsorption for 20 min

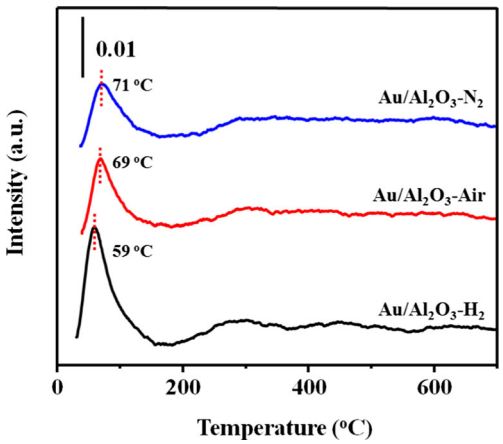

Fig. 6 The O_2-TPD profiles of Au/Al_2O_3 catalysts with different pretreatment atmospheres

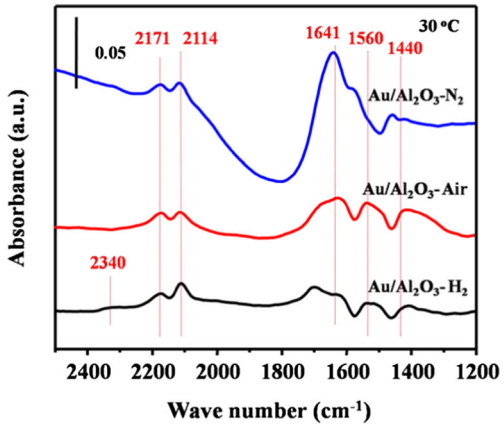

Fig. 7 In situ DRIFTS of various Au/Al_2O_3 catalysts after CO and O_2 co-adsorption for 20 min

weakly interacting with Au particles. For the Au/Al_2O_3-H_2 sample, the area of oxygen desorption was found to be higher than those of Au/Al_2O_3-air and Au/Al_2O_3-N_2 catalysts, suggesting that the Au/Al_2O_3-H_2 catalyst had more active oxygen species. It is known that the oxygen desorption behavior depends on the amount and strength of chemisorbed oxygen species which are easily desorbed at low temperature [40, 41]. A shift of the oxygen desorption peak to the lower temperature indicates an effective way to achieve lower reaction energy for CO oxidation and higher catalytic activity. The above results are in agreement with the catalytic activities (Fig. 2).

In situ DRIFTS analysis of the Au/Al_2O_3 catalyst

In order to explain the difference between catalytic behaviors of various Au/Al_2O_3 catalysts, in situ DRIFTS analysis was tested under CO oxidation conditions at 30 °C. As shown in Fig. 7, the surfaces of Au/Al_2O_3-N_2 and Au/Al_2O_3-air catalysts were mainly covered by carbonate-like species (1400–1800 cm^{-1}) with CO and O_2 co-adsorption for 20 min. This implies that carbonate-like species were easily accumulated on the surface of these catalysts at 30 °C. In contrast, few carbonate-like species were accumulated on the Au/Al_2O_3-H_2 catalyst surface. Simultaneously, a new band appeared at 2340 cm^{-1} which could be ascribed to CO_2 adsorbed on the Au/Al_2O_3-H_2 catalyst [42, 43], suggesting that CO can be oxidized into CO_2 products at 30 °C on the H_2-pretreated

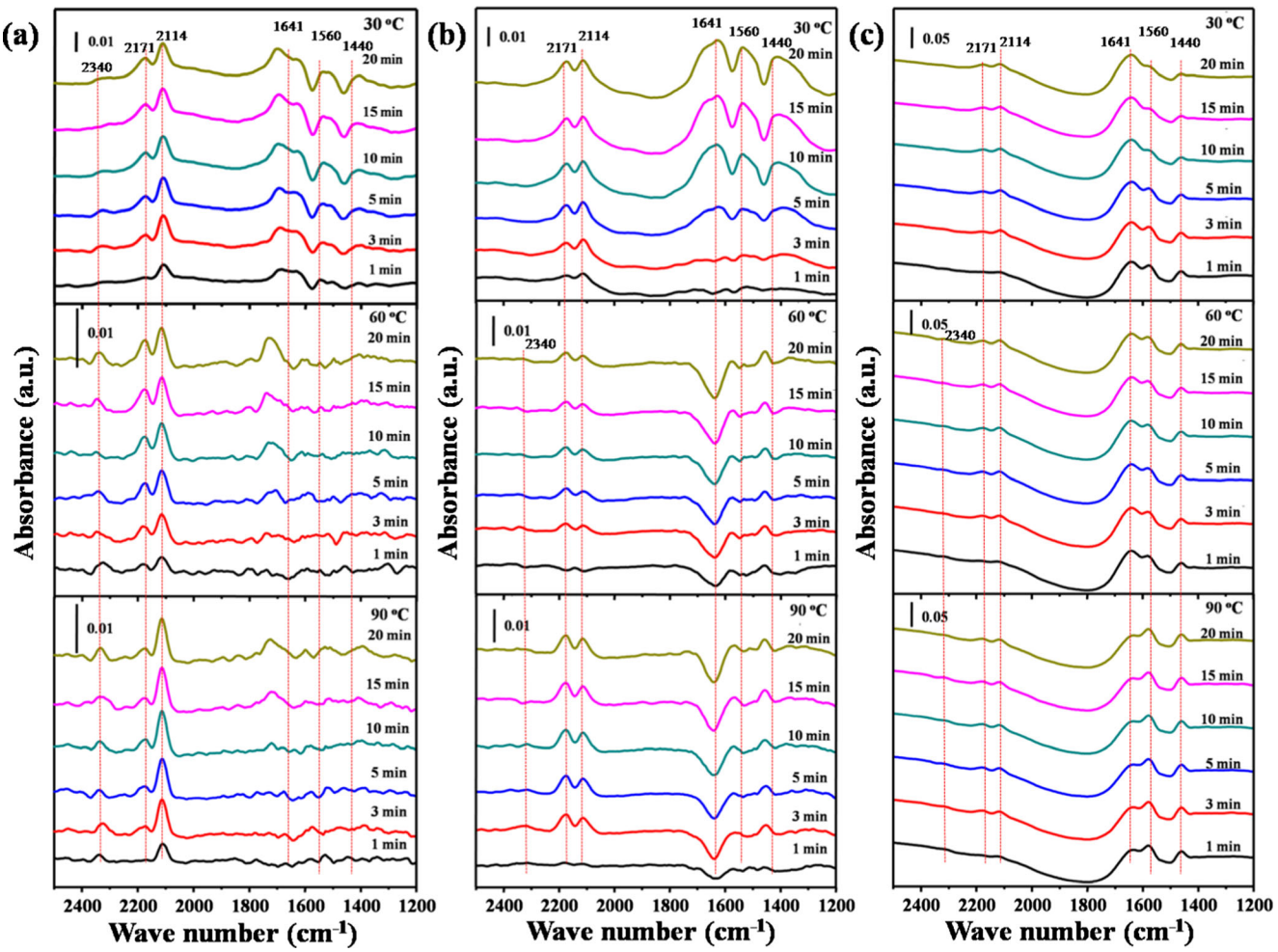

Fig. 8 In situ DRIFTS of the Au/Al_2O_3 catalysts for CO reaction at 30, 60, and 90 °C. **a** Au/Al_2O_3-H_2. **b** Au/Al_2O_3-air. **c** Au/Al_2O_3-N_2

catalyst. However, the CO_2 adsorption bands were not obvious for Au/Al_2O_3-N_2 and Au/Al_2O_3-air catalysts.

At 30 °C under CO oxidation conditions, the Au/Al_2O_3 catalyst surface is covered with CO, CO_2, and carbonate-like species. Comparing with the CO-DRIFTS in Fig. 5, the intensity of CO adsorption bands at 2171 and 2114 cm^{-1} decreased and the bands at 2056 cm^{-1} disappeared in the CO and O_2 co-adsorbed DRIFTS. A similar adsorption process was also reported by Liu et al. [44] with the Au-Cu/SBA-15 catalyst and was interpreted as the O_2 participating in the CO oxidation reaction, suggesting that the CO adsorbed on Au^0 readily reacts with O_2 even at a low temperature. This result indicates that the O_2 adsorption competes with CO on the catalyst surface. The intensity of peaks at 2114 cm^{-1} on various Au/Al_2O_3 catalysts with different pretreatment atmospheres follows the order of Au/Al_2O_3-H_2>Au/Al_2O_3-air>Au/Al_2O_3-N_2, which is consistent with their catalytic activities (Fig. 2).

To investigate the accumulation of adsorbed surface species during the reaction, we recorded the in situ DRIFTS experiments at high temperature. As shown in Fig. 8, the CO-derived species formed at 60 and 90 °C on the surface of the Au/Al_2O_3 catalysts are similar to those formed at 30 °C. Furthermore, the coverage of the $Au^{\delta+}/Au^0$–CO (the bands at 2171 and 2114 cm^{-1}) species decreased remarkably with temperature increasing. The intensity of the main carbonyl band ($Au^{\delta+}/Au^0$–CO) increases with time. Figure 8a shows that the Au/Al_2O_3-H_2 catalyst reached equilibrium of CO adsorption/desorption after 10 min. However, the Au/Al_2O_3-air and Au/Al_2O_3-N_2 catalysts reached equilibrium for CO adsorption/desorption after 15 min (Fig. 8b, c). These results suggest that the CO adsorption rate is higher on the surface of the Au/Al_2O_3-H_2 catalyst and thus contributes an excellent catalytic activity.

Additionally, Fig. 8 shows that the intensity of the adsorption band assigned to $Au^{\delta+}/Au^0$–CO (2171 and 2114 cm^{-1}) decreased when the CO oxidation temperature was raised from 30 to 90 °C. Meanwhile, the intensity of the CO_2 peak increased. This result indicates that all Au/Al_2O_3 catalysts are reactive in the CO oxidation at 60 and 90 °C. In our work, the Au/Al_2O_3-H_2 catalyst is more active as shown by the stronger intensity of the CO_2 absorption band at 2340 cm^{-1} (Fig. 8). On the other hand, the peak intensity of carbonate-like species over the Au/Al_2O_3-H_2 and Au/Al_2O_3-air catalysts was lower at 60 and 90 °C, indicating that the adsorption on the catalyst was reversible at this temperature (Fig. 8a, b). In contrast, the inferior activity and rapid deactivation of the Au/Al_2O_3-N_2 catalyst can be well understood by the continuous accumulation of carbonate-like species with CO and O_2 co-adsorption tested at 90 °C (Fig. 8c). This is in good agreement with the catalytic activities. The presence of water vapor can enhance the catalytic activities due to the promotion of the decomposition of carbonate-like species (Fig. 3b), which is consistent with the literature conclusions [6]. These results in both O_2-TPD and in situ DRIFTS measurements well explain why the catalyst pretreated under H_2 atmosphere displays a higher activity and stability in CO oxidation (Fig. 3a, d).

Conclusions

The influence of pretreatment atmospheres on the surface properties and catalytic performances of Au/Al_2O_3 catalysts was investigated. The low-temperature CO oxidation activity of various Au/Al_2O_3 catalysts was found to be Au/Al_2O_3-H_2> Au/Al_2O_3-air>Au/Al_2O_3-N_2. The catalyst pretreated under a H_2 atmosphere shows excellent catalytic activity and stability in the co-presence of CO_2 and H_2O at room temperature. The O_2-TPD and in situ DRIFTS results revealed that the Au/Al_2O_3-H_2 catalyst greatly enhanced the CO adsorption capacity and facilitated the oxygen activation. The deactivation observed on Au/Al_2O_3 catalysts was caused by adsorption of carbonate-like species. As compared with the Au/Al_2O_3-N_2 sample, the superior stability of the Au/Al_2O_3-H_2 catalyst may result from its suppressed accumulation of carbonate-like species under the co-presence of H_2O vapor and CO_2.

Acknowledgments This work was supported by the National Program on Key Basic Research Project (No. 2013CB934104).

References

1. Hashmi ASK, Hutchings GJ (2006) Gold catalysis. Angew Chem Int Ed 45:7896–7936
2. Haruta M, Yamada N, Kobayashi T, Iijima S (1989) Gold catalysts prepared by coprecipitation for low-temperature oxidation of hydrogen and of carbon monoxide. J Catal 115:301–309
3. Haruta M, Tsubota S, Kobayashi T, Kageyama H, Genet MJ, Delmon B (1993) Low-temperature oxidation of CO over gold supported on TiO_2, α-Fe_2O_3, and Co_3O_4. J Catal 144:175–192
4. Okumura M, Nakamura S, Tsubota S, Nakamura T, Azuma M, Haruta M (1998) Chemical vapor deposition of gold on Al_2O_3, SiO_2, and TiO_2 for the oxidation of CO and of H_2. Catal Lett 51: 53–58
5. Cunningham DAH, Vogel W, Haruta M (1999) Negative activation energies in CO oxidation over an icosahedral $Au/Mg(OH)_2$ catalyst. Catal Lett 63:43–47
6. Daté M, Okumura M, Tsubota S, Haruta M (2004) Vital role of moisture in the catalytic activity of supported gold nanoparticles. Angew Chem Int Ed 43:2129–2132
7. Tabakova T, Ilieva L, Ivanov I, Zanella R, Sobczak JW, Lisowski W, Kaszkur Z, Andreeva D (2013) Influence of the preparation method and dopants nature on the WGS activity of gold catalysts supported on doped by transition metals ceria. Appl Catal B Environ 136–137: 70–80

8. Haruta M, Ueda A, Tsubota S, Sanchez RMT (1996) Low-temperature catalytic combustion of methanol and its decomposed derivatives over supported gold catalysts. Catal Today 29:443–447
9. Long J, Liu H, Wu SJ, Liao S, Li Y (2013) Selective oxidation of saturated hydrocarbons using Au-Pd alloy nanoparticles supported on metal-organic frameworks. ACS Catal 3:647–654
10. Valden M, Lai X, Goodman DW (1998) Onset of catalytic activity of gold clusters on titania with the appearance of nonmetallic properties. Science 281:1647–1650
11. Hughes MD, Xu YJ, Jenkins P, McMorn P, Landon P, Enache DI, Carley AF, Attard GA, Hutchings GJ, King F, Stitt EH, Johnston P, Griffin K, Kiely CJ (2005) Tunable gold catalysts for selective hydrocarbon oxidation under mild conditions. Nature 437:1132–1135
12. Corma A, Serna P (2006) Chemoselective hydrogenation of nitro compounds with supported gold catalysts. Science 313:332–334
13. Li L, Wang A, Qiao B, Lin J, Huang Y, Wang X, Zhang T (2013) Origin of the high activity of Au/FeO_x for low-temperature CO oxidation: direct evidence for a redox mechanism. J Catal 299:90–100
14. Li WC, Comotti M, Schüth F (2006) Highly reproducible syntheses of active Au/TiO_2 catalysts for CO oxidation by deposition-precipitation or impregnation. J Catal 237:190–196
15. Carrettin S, Concepción P, Corma A, Nieto JML, Puntes VF (2004) Nanocrystalline CeO_2 increases the activity of Au for CO oxidation by two orders of magnitude. Angew Chem Int Ed 43:2538–2540
16. Zhang Y, Zhaorigetu B, Jia M, Chen C, Zhao J (2013) Clay-based SiO_2 as active support of gold nanoparticles for CO oxidation catalyst: pivotal role of residual Al. Catal Commun 35:72–75
17. Wen L, Fu JK, Gu PY, Yao BX, Lin ZH, Zhou JZ (2008) Monodispersed gold nanoparticles supported on γ-Al_2O_3 for enhancement of low-temperature catalytic oxidation of CO. Appl Catal B Environ 79:402–409
18. Schubert MM, Hackenberg S, Veen ACV, Muhler M, Plzak V, Behm RJ (2001) CO oxidation over supported gold catalysts-"inert" and "active" support materials and their role for the oxygen supply during reaction. J Catal 197:113–122
19. Wang J, Lu AH, Li MR, Zhang WP, Chen YS, Tian DX, Li WC (2013) Thin porous alumina sheets as supports for stabilizing gold nanoparticles. ACS Nano 7:4902–4910
20. Comotti M, Li WC, Spliethoff B, Schüth F (2006) Support effect in high activity gold catalysts for CO oxidation. J Am Chem Soc 128:917–924
21. Wang GH, Li WC, Jia KM, Spliethoff B, Schüth F, Lu AH (2009) Shape and size controlled α-Fe_2O_3 nanoparticles as supports for gold-catalysts: synthesis and influence of support shape and size on catalytic performance. Appl Catal A Gen 364:42–47
22. Park ED, Lee JS (1999) Effects of pretreatment conditions on CO oxidation over supported Au catalysts. J Catal 186:1–11
23. Szabó EG, Tompos A, Hegedűs M, Szegedi Á, Margitfalvi JL (2007) The influence of cooling atmosphere after reduction on the catalytic properties of Au/Al_2O_3 and Au/MgO catalysts in CO oxidation. Appl Catal A Gen 320:114–121
24. Wang LC, He L, Liu YM, Cao Y, He HY, Fan KN, Zhuang JH (2009) Effect of pretreatment atmosphere on CO oxidation over α-Mn_2O_3 supported gold catalysts. J Catal 264:145–153
25. Xu X, Fu Q, Guo X, Bao X (2013) A highly active "NiO-on-Au" surface architecture for CO oxidation. ACS Catal 3:1810–1818
26. Zhang RR, Ren LH, Lu AH, Li WC (2011) Influence of pretreatment atmospheres on the activity of Au/CeO_2 catalyst for low-temperature CO oxidation. Catal Commun 13:18–21
27. Wang J, Hu ZH, Miao YX, Li WC (2014) Hollow γ-Al_2O_3 microspheres as highly "active" supports for Au nanoparticle catalysts in CO oxidation. Gold Bull 47:95–101
28. An AF, Lu AH, Sun Q, Wang J, Li WC (2011) Gold nanoparticles stabilized by a flake-like Al_2O_3 support. Gold Bull 44:217–222
29. Han YF, Zhong ZY, Ramesh K, Chen FX, Chen LW (2007) Effects of different types of γ-Al_2O_3 on the activity of gold nanoparticles for CO oxidation at low-temperatures. J Phys Chem C 111:3163–3170
30. Lee SJ, Gavriilidis A (2002) Supported Au catalysts for low-temperature CO oxidation prepared by impregnation. J Catal 206:305–313
31. Qi C, Zhu S, Su H, Lin H, Guan R (2013) Stability improvement of Au/Fe-La-Al_2O_3 catalyst via incorporating with a Fe_xO_y layer in CO oxidation process. Appl Catal B Environ 138–139:104–112
32. Zou X, Xu J, Qi S, Suo Z, An L, Li F (2011) Effects of preparation conditions of $Au/FeO_x/Al_2O_3$ catalysts prepared by a modified two-step method on the stability for CO oxidation. J Nat Gas Chem 20:41–47
33. Wang X, Lu G, Guo Y, Zhang Z, Guo Y (2011) Role of Rh promoter on increasing stability of Au/Al_2O_3 catalyst for CO oxidation at low temperature. Environ Chem Lett 9:185–189
34. Shang C, Liu ZP (2010) Is transition metal oxide a must? Moisture-assisted oxygen activation in CO oxidation on gold/γ-alumina. J Phys Chem C 114:16989–16995
35. Piccolo L, Daly H, Valcarcel A, Meunier FC (2009) Promotional effect of H_2 on CO oxidation over Au/TiO_2 studied by operando infrared spectroscopy. Appl Catal B Environ 86:190–195
36. Leba A, Davran CT, Önsan ZI, Yıldırım R (2012) DRIFTS study of selective CO oxidation over Au/γ-Al_2O_3 catalyst. Catal Commun 29:6–10
37. Liu X, Liu MH, Luo YC, Mou CY, Lin SD, Cheng H, Chen JM, Lee JF, Lin TS (2012) Strong metal-support interactions between gold nanoparticles and ZnO nanorods in CO oxidation. J Am Chem Soc 134:10251–10258
38. Chakarova K, Mihaylov M, Ivanova S, Centeno MA, Hadjiivanov K (2011) Well-defined negatively charged gold carbonyls on Au/SiO_2. J Phys Chem C 115:21273–21282
39. Venkov T, Klimev H, Centeno MA, Odriozola JA, Hadjiivanov K (2006) State of gold on an Au/Al_2O_3 catalyst subjected to different pre-treatments: an FTIR study. Catal Commun 7:308–313
40. Wang YZ, Zhao YX, Gao CG, Liu DS (2008) Origin of the high activity and stability of Co_3O_4 in low-temperature CO oxidation. Catal Lett 125:134–138
41. Xu H, Li W, Shang S, Yan C (2011) Influence of MgO contents on silica supported nano-size gold catalyst for carbon monoxide total oxidation. J Nat Gas Chem 20:498–502
42. Schumacher B, Denkwitz Y, Plzak V, Kinne M, Behm RJ (2004) Kinetics, mechanism, and the influence of H_2 on the CO oxidation reaction on a Au/TiO_2 catalyst. J Catal 224:449–462
43. Denkwitz Y, Makosch M, Geserick J, Hörmann U, Selve S, Kaiser U, Hüsing N, Behm RJ (2009) Influence of the crystalline phase and surface area of the TiO_2 support on the CO oxidation activity of mesoporous Au/TiO_2 catalysts. Appl Catal B Environ 91:470–480
44. Liu X, Wang A, Li L, Zhang T, Mou CY, Lee JF (2011) Structural changes of Au-Cu bimetallic catalysts in CO oxidation: in situ XRD, EPR, XANES, and FT-IR characterizations. J Catal 278:288–296